Characteristic X-Ray Production in the M Shell of $_{60}$Nd, $_{62}$Sm, $_{64}$Gd, $_{65}$Tb, $_{66}$Dy, and $_{67}$Ho by 25- to 100-keV Protons*

J. M. KHAN, D. L. POTTER, AND R. D. WORLEY
Lawrence Radiation Laboratory, University of California, Livermore, California
(Received 24 February 1964)

Characteristic M-shell x rays produced when protons of 25- to 100-keV energy are stopped in thick targets of $_{60}$Nd, $_{62}$Sm, $_{64}$Gd, $_{65}$Tb, $_{66}$Dy, and $_{67}$Ho have been observed by proportional-counter detection. The energy of the x rays (M_α) varied from 980 to 1360 eV. The quantities obtained in the experiment were the thick-target yields (x rays per proton) and estimates of the x-ray production and ionization cross sections. With a fluorescence yield of 0.01, the ionization cross sections fall between 10^{-24} and 10^{-21} cm^2.

INTRODUCTION

ATOMIC ionization by heavy charged particles has been studied in a number of contexts. Early work centered upon evaluation of the average stopping power of materials for high-energy protons and alpha particles (in the MeV range).[1] These effects have also been investigated during the process of nuclear excitation experiments, as they represent background radiations emitted by the targets. In addition, specific experiments have been performed to measure the ionization cross section in the various atomic shells (K,L,M).[2–9] As techniques have improved, the measurements have been extended to lower bombarding energies (60 keV) and to the detection of x rays of lower energy (1 keV).[10–12]

In the present experiment measurements have been made of the thick-target yield (x rays per proton) from the M shell of six rare-earth elements (Nd, Sm, Gd, Tb, Dy, and Ho) produced by protons of energy 25 to 100 keV. From these thick-target yields and estimates of the stopping power of the material for the protons, self-absorption of the elements for their own characteristic x rays, and fluorescence yields, it is possible to obtain the ionization cross section.

At the present time there are no theoretical predictions of these M-shell cross sections available for comparison. However, for K shells of a number of elements predictions have been made.[9] These fall into two categories. The early calculations were based upon a Born-approximation description of the proton trajectory, which is most appropriate for higher bombarding energies ($\geq$0.5 MeV). These predicted values are higher than the observed at energies less than 0.5 MeV. More recently the calculations have been repeated employing a deflected trajectory. The results of this calculation have represented a considerable improvement.[13]

EXPERIMENTAL APPARATUS AND METHOD

The experimental system consists of (1) proton source (electrodeless discharge); (2) accelerating column (dc); (3) analyzing magnet; (4) collimating structure; (5) target chamber (45° incidence upon target sample); (6) proportional counter (at 90° to beam) and associated electronics to discriminate against noise and to count signal pulses. The details of the apparatus and method have been given in previous publications and will not be given here.[10,11]

The energy of the protons was determined by measurement of the total potential drop from the probe voltage in the source tube to the target (at ground potential). This was accomplished by use of a precision resistor string (with frequent calibrations). The analyzing magnet served only to separate the protons from the other ion components produced in the source. The target chamber consisted of a target support rod surrounded by an electron shield. These were appropriately biased and both were included in the current measuring system. Care was taken to avoid errors due to target surface contamination. The proportional counter is of conventional design (2 in. i.d.$\times$12 in. length with a 0.003-in. stainless-steel center wire). The counter was used in a flow mode at atmospheric pressure (P-10 gas: 90% argon, 10% methane). The output signals of the counter were monitored by a pulse-height analyzer in coincidence with the output of a differential discriminator. An absorber foil changer was employed to evaluate the absorption in the 0.0004-in. aluminum counter window.

* Work performed under the auspices of the U. S. Atomic Energy Commission.
[1] See, for example, J. Lindhard and M. Scharff, Kgl. Danske Videnskab. Selskab, Mat. Fys. Medd. **27**, No. 15 (1953); and W. Whaling, *Nuclear Spectroscopy* (Academic Press Inc., New York, 1960), Part A, Chap. I.
[2] C. Gerthsen and W. Reusse, Z. Physik **34**, 478 (1933).
[3] O. Peter, Ann. Physik **27**, 299 (1936).
[4] H. W. Lewis, F. Genevese, and E. J. Konopinski, Phys. Rev. **51**, 835 (1957).
[5] H. W. Lewis, B. E. Simmons, and E. Merzbacher, Phys. Rev. **91**, 943 (1953).
[6] P. R. Berington and E. M. Bernstein, Bull. Am. Phys. Soc. **1**, 198 (1956).
[7] E. M. Bernstein and H. W. Lewis, Phys. Rev. **95**, 83 (1953).
[8] R. C. Jopson, Hans Mark, and C. D. Swift, Phys. Rev. **127**, 1612 (1962).
[9] For a general review of experimental and theoretical work see E. Merzbacher and H. W. Lewis, in *Handbuch der Physik*, edited by S. Flügge (Springer-Verlag, Berlin, 1958), Vol. 34, p. 166.
[10] J. M. Khan and D. L. Potter, Phys. Rev. **133**, A890 (1964).
[11] J. M. Khan, D. L. Potter, and R. D. Worley, Phys. Rev. **134**, A320 (1964).
[12] J. M. Khan, D. L. Potter, and R. D. Worley (to be published).
[13] J. Bang and J. M. Hansten, Kgl. Danske Videnskab. Selskab, Mat. Fys. Medd. **31**, No. 13 (1959).

TABLE I. Thick-target yields, production, and ionization cross sections in the M shell.

Element	Z	E_p (keV)	$N(E)$ (x rays per μC before geometrical and absorption correction)	I_μ[a] ($\pm 15\%$) (x rays/proton)	$\frac{dI_\mu}{dE}$ (x rays/proton/keV)	$S(E)$[b] (keV-cm^2/mg)	$\frac{1}{n}\frac{dI}{dE}\cdot S(E)$ (cm^2)	$\frac{\mu}{\rho n} I_\mu$ (cm^2)	σ_x (cm^2)	σI[c] (cm^2)
Neodymium	60	25	0.15	1.26×10^{-9}	0.97×10^{-9}	55	1.29×10^{-26}	1.52×10^{-27}	1.44×10^{-26}	1.44×10^{-24}
$h\nu(M_\alpha)\doteq 980$ eV		30	0.86	7.21×10^{-9}	1.84×10^{-9}	66	2.92×10^{-26}	8.68×10^{-27}	3.79×10^{-26}	3.79×10^{-24}
$\frac{1}{n}=2.41\times10^{-19}$ mg/atom		40	7.40	6.20×10^{-8}	1.24×10^{-8}	88	2.63×10^{-25}	7.47×10^{-26}	3.38×10^{-25}	3.38×10^{-23}
		50	26.9	2.25×10^{-7}	2.16×10^{-8}	110	5.74×10^{-25}	2.71×10^{-25}	8.45×10^{-25}	8.45×10^{-23}
$\frac{\mu^d}{\rho}=5$ cm^2/mg		60	63.0	5.28×10^{-7}	3.73×10^{-8}	110	9.88×10^{-25}	6.36×10^{-25}	1.62×10^{-24}	1.62×10^{-22}
		70	118	9.89×10^{-7}	5.85×10^{-8}	110	1.55×10^{-24}	1.19×10^{-24}	2.74×10^{-24}	2.74×10^{-22}
$\bar{\omega}^e=0.01$		80	191	1.60×10^{-6}	7.30×10^{-8}	110	1.94×10^{-24}	1.93×10^{-24}	3.87×10^{-24}	3.87×10^{-22}
T_w[a] $=0.064$		90	293	2.46×10^{-6}	8.38×10^{-8}	110	2.22×10^{-24}	2.96×10^{-24}	5.18×10^{-24}	5.18×10^{-22}
		100	409	3.43×10^{-6}	8.31×10^{-8}	110	2.20×10^{-24}	4.13×10^{-24}	6.33×10^{-24}	6.33×10^{-22}
Samarium	62	25	<0.1	$<0.6\times10^{-9}$	$<0.5\times10^{-9}$	55	$<0.6\times10^{-26}$	$<0.8\times10^{-27}$	$<0.7\times10^{-26}$	$<0.7\times10^{-24}$
$h\nu(M_\alpha)\doteq 1090$ eV		30	1.10	6.39×10^{-9}	1.84×10^{-9}	66	3.07×10^{-26}	8.08×10^{-27}	3.88×10^{-26}	3.88×10^{-24}
$\frac{1}{n}=2.53\times10^{-19}$ mg/atom		40	11.3	6.57×10^{-8}	1.15×10^{-8}	88	2.55×10^{-25}	8.31×10^{-26}	3.38×10^{-25}	3.38×10^{-23}
		50	45.0	2.61×10^{-7}	3.34×10^{-8}	110	9.29×10^{-25}	3.30×10^{-25}	1.26×10^{-24}	1.26×10^{-22}
$\frac{\mu^d}{\rho}=5$ cm^2/mg		60	118	6.86×10^{-7}	5.28×10^{-8}	110	1.47×10^{-24}	8.68×10^{-25}	2.34×10^{-24}	2.34×10^{-22}
		70	228	1.32×10^{-6}	7.78×10^{-8}	110	2.16×10^{-24}	1.67×10^{-24}	3.83×10^{-24}	3.83×10^{-22}
$\bar{\omega}^e=0.01$		80	387	2.25×10^{-6}	1.05×10^{-7}	110	2.92×10^{-24}	2.85×10^{-24}	5.77×10^{-24}	5.77×10^{-22}
T_w[a] $=0.093$		90	585	3.40×10^{-6}	1.37×10^{-7}	110	3.81×10^{-24}	4.30×10^{-24}	8.11×10^{-24}	8.11×10^{-22}
		100	830	4.82×10^{-6}	1.72×10^{-7}	110	4.78×10^{-24}	6.10×10^{-24}	1.09×10^{-23}	1.09×10^{-21}
Gadolinium	64	25	<0.1	$<0.4\times10^{-9}$						
$h\nu(M_\alpha)\doteq 1190$ eV		30	1.15	4.43×10^{-9}	1.36×10^{-9}	66	2.33×10^{-26}	5.76×10^{-27}	2.91×10^{-26}	2.91×10^{-24}
$\frac{1}{n}=2.60\times10^{-19}$ mg/atom		40	14.0	5.39×10^{-8}	9.56×10^{-9}	88	2.19×10^{-25}	7.01×10^{-26}	2.89×10^{-25}	2.89×10^{-23}
		50	64.5	2.48×10^{-7}	3.36×10^{-8}	110	9.61×10^{-25}	3.22×10^{-25}	1.28×10^{-24}	1.28×10^{-22}
$\frac{\mu^d}{\rho}=5$ cm^2/mg		60	177	6.81×10^{-7}	6.15×10^{-8}	110	1.76×10^{-24}	8.85×10^{-25}	2.64×10^{-24}	2.64×10^{-22}
		70	365	1.42×10^{-6}	8.84×10^{-8}	110	2.53×10^{-24}	1.85×10^{-24}	4.38×10^{-24}	4.38×10^{-22}
$\bar{\omega}^e=0.01$		80	640	2.46×10^{-6}	1.29×10^{-7}	110	3.69×10^{-24}	3.20×10^{-24}	6.89×10^{-24}	6.89×10^{-22}
T_w[a] $=0.14$		90	1010	3.89×10^{-6}	1.64×10^{-7}	110	4.69×10^{-24}	5.06×10^{-24}	9.75×10^{-24}	9.75×10^{-22}
		100	1470	5.66×10^{-6}	1.78×10^{-7}	110	5.09×10^{-24}	7.36×10^{-24}	1.24×10^{-23}	1.24×10^{-21}
Terbium	65	25	<0.16	$<0.5\times10^{-9}$						
$h\nu(M_\alpha)\doteq 1250$ eV		30	1.04	3.22×10^{-9}	1.14×10^{-9}	66	1.98×10^{-26}	4.25×10^{-27}	2.41×10^{-26}	2.41×10^{-24}
$\frac{1}{n}=2.64\times10^{-19}$ mg/atom		40	14.5	4.51×10^{-8}	7.69×10^{-9}	88	1.78×10^{-25}	5.95×10^{-25}	2.37×10^{-25}	2.37×10^{-23}
		50	72.1	2.23×10^{-7}	3.02×10^{-8}	110	8.76×10^{-25}	2.94×10^{-25}	1.17×10^{-24}	1.17×10^{-22}
$\frac{\mu^d}{\rho}=5$ cm^2/mg		60	203	6.29×10^{-7}	5.69×10^{-8}	110	1.65×10^{-24}	8.30×10^{-24}	2.48×10^{-24}	2.48×10^{-22}
		70	430	1.33×10^{-6}	8.75×10^{-8}	110	2.54×10^{-24}	1.76×10^{-24}	4.30×10^{-24}	4.30×10^{-22}
$\bar{\omega}^e=0.01$		80	770	2.39×10^{-6}	1.22×10^{-7}	110	3.54×10^{-24}	3.15×10^{-24}	6.69×10^{-24}	6.69×10^{-22}
T_w[a] $=0.174$		90	1200	3.72×10^{-6}	1.56×10^{-7}	110	4.52×10^{-24}	4.91×10^{-24}	9.43×10^{-24}	9.43×10^{-22}
		100	1700	5.49×10^{-6}	1.75×10^{-7}	110	5.08×10^{-24}	7.25×10^{-24}	1.23×10^{-23}	1.23×10^{-21}
Dysprosium	66	30	1.00	2.62×10^{-9}	0.86×10^{-9}	66	1.52×10^{-26}	3.52×10^{-27}	1.87×10^{-26}	1.87×10^{-24}
$h\nu(M_\alpha)\doteq 1300$ eV		40	14.7	3.85×10^{-8}	6.58×10^{-9}	88	1.56×10^{-25}	5.18×10^{-26}	2.08×10^{-25}	2.08×10^{-23}
$\frac{1}{n}=2.69\times10^{-19}$ mg/atom		50	78	2.04×10^{-7}	2.86×10^{-8}	110	8.47×10^{-25}	2.74×10^{-25}	1.12×10^{-24}	1.12×10^{-22}
		60	240	6.28×10^{-7}	5.78×10^{-8}	110	1.71×10^{-24}	8.45×10^{-25}	2.56×10^{-24}	2.56×10^{-22}
$\frac{\mu^d}{\rho}=5$ cm^2/mg		70	520	1.36×10^{-6}	8.70×10^{-8}	110	2.58×10^{-24}	1.83×10^{-24}	4.41×10^{-24}	4.41×10^{-22}
		80	935	2.45×10^{-6}	1.33×10^{-7}	110	3.93×10^{-24}	3.42×10^{-24}	7.35×10^{-24}	7.35×10^{-22}
$\bar{\omega}^e=0.01$		90	1520	3.98×10^{-6}	1.76×10^{-7}	110	5.21×10^{-24}	5.35×10^{-24}	1.06×10^{-23}	1.06×10^{-21}
T_w[a] $=0.206$		100	2230	5.84×10^{-6}	2.05×10^{-7}	110	6.07×10^{-24}	7.85×10^{-24}	1.39×10^{-23}	1.39×10^{-21}
Holmium	67	30	0.78	1.75×10^{-9}	0.67×10^{-9}	66	1.21×10^{-26}	2.40×10^{-27}	1.45×10^{-26}	1.45×10^{-24}
$h\nu(M_\alpha)\doteq 1360$ eV		40	14.3	3.20×10^{-8}	6.29×10^{-9}	88	1.52×10^{-25}	4.38×10^{-26}	1.96×10^{-25}	1.96×10^{-23}
$\frac{1}{n}=2.74\times10^{-19}$ mg/atom		50	81.6	1.83×10^{-7}	2.62×10^{-8}	110	7.89×10^{-25}	2.51×10^{-25}	1.04×10^{-24}	1.04×10^{-22}
		60	251	5.62×10^{-7}	4.88×10^{-8}	110	1.47×10^{-24}	7.70×10^{-25}	2.24×10^{-24}	2.24×10^{-22}
$\frac{\mu^d}{\rho}=5$ cm^2/mg		70	569	1.27×10^{-6}	8.73×10^{-8}	110	2.63×10^{-24}	1.74×10^{-24}	4.37×10^{-24}	4.37×10^{-22}
		80	1046	2.34×10^{-6}	1.28×10^{-7}	110	3.86×10^{-24}	3.21×10^{-24}	7.07×10^{-24}	7.07×10^{-22}
		90	1720	3.85×10^{-6}	1.77×10^{-7}	110	5.33×10^{-24}	5.27×10^{-24}	1.06×10^{-23}	1.06×10^{-21}
$\bar{\omega}^e=0.01$		100	2578	5.77×10^{-6}	2.01×10^{-7}	110	6.05×10^{-24}	7.90×10^{-24}	1.40×10^{-23}	1.40×10^{-21}
T_w[a] $=0.241$										

[a] $I_\mu=\Lambda/T_w N(E)$. $\Lambda\equiv$geometrical factor $=3364$, $T_w=$counter-window transmission factor. Error on all 25-keV values $=\pm 50\%$.
[b] S. D. Warshaw and S. K. Allison, Rev. Mod. Phys. **25**, 779 (1953).
[c] In view of the uncertainties in the values of $S(E)$, μ/ρ, and $\bar{\omega}$ these numbers are good to a factor of 5.
[d] Extrapolation: *Handbook of Chemistry and Physics* (Chemical Rubber Publishing Company, Cleveland, Ohio, 1962), 44th ed.
[e] Estimate: E. H. S. Burhop, *The Auger Effect and Other Radiationless Transitions* (Cambridge University Press, New York, 1952).

MEASUREMENTS

The x-ray-production cross section can be computed from the thick-target yield by using the formula[9]

$$\sigma_x(E_p)=-\frac{1}{n}\frac{dI_\mu}{dE}S(E_p)+\frac{1}{n}\left(\frac{\mu}{\rho}\right)I_\mu.$$

The ionization cross section is obtained by correcting this number for the radiationless reorganization of the atom:

$$\sigma_I(E_p)=(1/\bar{\omega})\sigma_x(E_p),$$

where $\bar{\omega}$ is the average fluorescence yield for the shell.

The application of this formula has a number of inherent difficulties when employed to evaluate the cross section for the L and M shells, particularly when these shells have characteristic radiations which have a broad spread in energy components. First, it is difficult to correct accurately for the absorption in the counter window, as the ratio of the components is altered. Secondly, the ratio of the component radiations changes as a function of the production depth (hence proton energy) due not only to the spread in energy but also due to internal absorption of the higher energy components by the less tightly bound levels of the same shell.[11] The results of the present experiment are given in Table I. The values assumed for the stopping power are extrapolated from the values presented by Allison and Warshaw. The μ/ρ self-absorption number is based upon extrapolation from the values of Allen.

DISCUSSION

In view of the lack of support data the ionization cross-section evaluations must be considered as qualitative (good to a factor of 5). There is most certainly a spread in the values of $S(E)$ and μ/ρ for the rare-earth elements. The fluorescent yields employed to obtain the ionization cross section from the production cross section are estimates only.

Several observations are of interest, however. The first is that although the binding energies of the M_V shells vary from 0.98 to 1.36 keV, the thick-target yields and production cross sections are surprisingly close in value. In contradistinction, when one compares, at a bombarding energy of 100 keV, the values of the thick-target yield of copper in the L shell and neodymium in the M shell [$E_{L_{III}}$(Cu)=0.935 keV; E_{M_V}(Nd)=0.984 keV],[11] one finds that the copper value is almost an order of magnitude larger.

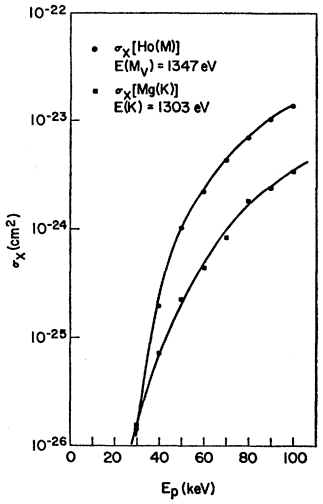

FIG. 1. Ho(M) and Mg(K) production cross section.

It is useful to compare the functional dependences of the production cross sections for x rays of comparable energy, but originating from different shells. Measurements have recently been made of the thick-target yield and production cross section of magnesium over the energy range considered here.[12] The binding energy of this K shell is 1303 eV. This is quite close to the value of the binding energy of the M_V level of holmium (1347 eV). The comparison of these two sets of data is made in Fig. 1. Holmium, with more electrons per atom available for ionization does appear to yield the greater number of x rays, at least above 30-keV proton energy. The dependence upon bombarding energy is much greater for the case of holmium, however.

The current set of experiments represents the first recent collection of data in these energy ranges. As a result, the systematics of the phenomena have not yet emerged. It has been shown that the Born approximation calculations in this bombarding energy region are in error by as much as two orders of magnitude (high) where experimental tests have been applied.[8,10,11] The deflected-trajectory calculations of Bang and Hansteen have not yet been applied to other than K shells, but seem desirable.